Proceedings of the Canadian Society for Mechanical Engineering International Congress 2021
CSME Congress 2021
June 27-30, 2021, Charlottetown, PE, Canada

EFFECT OF THE STRENGTH OF INDIVIDUAL STRUCTURES OF A 3D-PRINTED WC-Co CEMENTED CARBIDES ON ITS BULK MECHANICAL PROPERTIES

Joseph Agyapong[1], Solomon Boakye-Yiadom[1*], Aleksander Czekanski[1]
[1]Department of Mechanical Engineering, York University, Toronto, Canada
*e-mail address: sboakyey@yorku.ca

Abstract— The characterization of mechanical properties of a 3D printed cemented carbide has become one of the most important procedures aiding the fabrication of quality parts. For a material such as tungsten carbide cobalt (WC-Co) which are known for high hardness and fracture toughness, it is very important to consider the contribution of the matrix (WC) and binder (Co) separately. This is because, the volume fraction of these structures and its spatial distribution is what determines the bulk properties of the material. In this study, the strength of cemented carbides is determined with the aid of Quantitative Nanomechanical analysis module of the atomic force microscope (QNM-AFM). The correlation of this mechanical characterization is then linked to the microstructure of the material which was observed and obtained using scanning electron microscopy. It is observed that the microstructure of the WC-Co was characterized by three distinct structures namely: relatively large poly-angular chips, "eta phase"- and dark- background regions. The volume fraction and spatial distribution of these structures are the main contributors to the bulk properties of the material. It was observed that, the polyangular chips were the strongest structures present in the sample. The eta phase regions were observed to occupy almost 40% of the area of the sample. However, the "eta phase" regions had a relatively higher strength compared to the dark background regions. This information can be used qualitatively tailor the microstructures created in the sample through processing parameters and post processing parameters for specific applications. The versatility of the PF-QNM module of the Atomic Force Microscopy is also explored and recommended for nanoscale analysis of mechanical characterization of lightweight materials and complex microstructures like additively manufactured parts.

Keywords-component; Selective Laser Sintering; Cemented Carbides; Nanomechanical mapping, Heat Treatment; Metal 3D Printing

I. INTRODUCTION

Cemented carbides are used for making tools and molds because they are known to have high hardness and fracture toughness [1]. Other industries such as the nuclear, military and mining industries also employ this material for their dynamic and high temperature applications [2]. Cemented carbides constitute a ceramic matrix(carbide) and a binder which is usually a metal. The ceramic matrix contributes to the hardness of the material whereas the binder adds a level of ductility to the material [3]. Typically, two groups of cemented carbides can be distinguished, namely, by the size and volume fraction of matrix and the spatial distribution of the binder. A higher content of the matrix makes the cemented carbides more wear resistant because of the increase of both hardness (HV) and compressive strength [4]. In addition, the elastic Young's modulus (E) increases as well. In contrast, a higher proportion of a binding metal makes the cemented carbide tougher and causes the bending strength to increase. The main carbides used as the ceramic matrix can be tungsten carbide (WC), titanium carbide (TiC), tantalum carbide (TaC) or niobium carbide (NbC) [5]. The binder is mostly cobalt (Co) otherwise Ni or Fe can also be added for other added advantages such as non-corrosiveness of the material. The most common and widely used carbide is the WC because of its availability and hardness value compared to the other carbides. Due to its high melting point, powder metallurgy techniques have been the preferred methods used to process these materials. In fact, up unto this day, using this technique has proven successful but the WC-Co parts produced take a long processing time and a level of difficulty to create them [6]. However, research to adopt novel metal-additive manufacturing (M-AM) for cemented carbides is now taking way [7-10]. The technique eradicates the problem of being limited by intricacy of part being produced and shortens the time taken to produce it as well its unique part customization advantage. However, M-AM has also not yet been very responsive because it also presents some challenges at its onset. Microstructural defects such as porosity, micro cracks, residual stresses, and non-equilibrium phases have been prevalent in most of the materials that have been tried using the metal-additive manufacturing processes [6, 11, 12]. Currently, processing parameters optimization, powder customization and post processing treatments have been investigated and realized to aid in the mitigation or reduction in the major defects that this processing technique presents to the various parts printed [12]. For WC-Co, one major improvement suggested in the literature is a one-step post-processing treatment. This helps improve the mechanical properties of the material amidst minor microstructural defects observed in the printed parts. Kumar

conducted a study on adopting selective laser sintering and furnace heating for WC-17Co alloys to suggest a method of improvement. He concluded that the heat treatment would be a complementary processing technique for producing WC-17Co as it helped achieve better mechanical and wear properties [13]. Agyapong et al, also adopted the same heat treatment for SLS processed WC-17Co reinforced with hBN to improve the wear properties of the material. A general improvement in the mechanical and wear properties of the material was observed [14]. Other important studies adopted heat treatment for WC-Co used as coatings [15-17]. All these studies also proved the importance of heat treatment for the improvement of the wear properties.

However, most of these studies has very little extensive analysis on how these improvement form. Because WC-Co is a complex composite and determining the factors for improvement may be very difficult. Additionally, mechanical properties of materials are expected to differ from one microstructure to the other. These microstructures may differ due to the spatial distribution and volume fraction of the individual structures observed in WC-Co materials. This then influences the bulk properties of the material. Thus, individual measurement of the structures' properties may be an important factor to determine how the mechanical properties evolve during heat treatment and processing. However, traditional bulk measurements for mechanical properties on a lower scale are not microstructure sensitive and therefore not suitable for multi-faceted microstructure. In theory, atomic force microscopy (AFM) based techniques can be beneficial to address the study of the local properties of the material at nanoscale. AFM modes including force curve analysis and peak force quantitative nanomechanical (PF-QNM) analysis can be a proper technique to obtain local information on the microstructures to better explain the evolution of the properties. Also, due to the improved lateral resolution and capabilities in AFM, shallow indentations can also be performed and thus information on the morphological properties, stiffness, elastic properties, and modulus properties can be obtained. Therefore, local spatial variations due to heterogeneity of the microstructure can be observed. This is indeed important because the volume fraction and spatial distribution of these structures will contribute immensely to the bulk properties of the material. Thus, in this study, an interest in the nanomechanical characterization of the various structures of the samples are being investigated using AFM. The use of other advanced microscopy techniques is being employed to critically understand this correlation. The data will be indeed useful in the processing of cemented carbide (WC-Co) whereby a tailoring of the specific microstructure would therefore determine the desired bulk properties needed.

II. Ease of Use

A pre-alloyed powder which consists of 83wt.% WC and 17 wt.% Co was selected for this study based on initial parametric studies. An AM system, EOS M 280 used for selective laser sintering of processing customized metals was used for the processing of the WC-Co alloy powders. To avoid unwanted burning and oxidation during processing, the chamber was filled up with nitrogen gas during processing. For the part formed to fuse effectively on a small area of powder bed platform, an adaptive plate was used. A plate made of 1045 cold rolled steel acted as the substrate on which the samples were fabricated. Printing parameters that were fed into the AM system were adopted from a previous study as shown in Table 1 [18]. The AM system was equipped with a heater which heated the processing environment and adaptive plate up to 200 °C before processing the powders. These conditions were used to print samples of 5 mm thickness and a size of 20 mm x 50mm. The samples were sectioned into three part: one for microstructural studies, one for nanomechanical mapping and one more for micro hardness measurements. These three samples were cold mounted in epoxy resin without compromising the structure and composition of the samples. The mounted samples were prepared using piano flexible diamond disks with 5 different grades (80, 120, 240, 600 and 1200). During grinding, a maximum of 10 minutes was spent on each flexible diamond disk to obtain a smooth surface. This was followed by polishing the samples using monocrystalline diamond suspension (1 um, 0.5 um and 0.25 um) to obtain a mirror surface finish. The samples were not etched for this study. The microstructure of the polished samples was characterized using a scanning electron microscope (TESCAN VEGA 3) equipped with an energy dispersive spectroscopy (EDS) detector which was used to assess the chemical elements present in the samples. This analysis was to qualitatively determine the chemical elements that were present in the sample of the material after printing. Microhardness measurements were performed on the polished sample with a digital microhardness machine by applying a 300 gram-force (2.942N) for 15 seconds. A total of 25 hardness values (VHN) were recorded and their average values calculated as the hardness value of the sample. One sample was prepared adequately to be analyzed using the Bruker Multi Mode 8 AFM (York University). This machine offers a non-destructive way of assessing the nano mechanical properties of the material. Thus, it was used to analyze the qualitative nano mechanical mapping of the sample to visualize the elastic modulus distribution on the surface of the material. This was done using the Peak Force Quantitative Nanomechanical Mapping (PF QNM) mode in the software as well as using a custom-made cantilever with extremely high spring constant (2000 N/m) and diamond tip as an AFM probe. During acquisition of topographical and nano mechanical data, a constant peak force was adopted at low μN forces during experiments in order to obtain consistent data for the as-printed sample.

Table 1: Values for printing parameters

Parameter	**Value**
Laser Power	*270W*
Scan Speed	500mm/s
Beam diameter	0.1mm
Hatching distance	0.4mm
Layer thickness	0.04mm
Preheating	200 °C

III. RESULTS & DISCUSSION

Fig. 1 shows micrographs taken using the scanning electron microscope. These images are used to describe the microstructural features and structure of the as-printed WC-Co sample. In general, three distinct microstructural features were observed within the as-printed sample. These included irregular and regular poly-angular chips, "eta phase" regions and dark background regions. Fig. 1(a) shows the regular and irregular poly-angular chips observed on the as-printed sample. Typically, the sizes of the regular poly-angular chips were relatively small when compared to the irregular poly-angular chips. In addition, the surfaces of the regular poly-angular chips appeared to be relatively smooth with no strips or stringers while the irregular poly-angular chips had thin dark stringers on them as shown in Fig 1(b). There were also other areas that were purely dark in nature which were situated in regions around the polyangular chips. They were labelled as dark background regions (Fig. 1b). The observed "eta phase" regions were located at different areas of the sample occupying about 40% of the volume fraction after image processing and calculations (Fig. 1(a, c, d). On these regions, clusters of dark spots were usually observed on them as shown in Fig. 1(c). This was later identified as micro pores. Besides the pores, micro-cracks were also observed in the as-printed sample (Fig. 1(c)). These micro-cracks had branches of cracks with clusters of pores around them as shown in Fig. 1(c). Furthermore, some regions of the sample had agglomerations of tiny chips as shown in Fig. 1(d). These agglomerations of tiny chips were usually observed around the "eta phase" regions.

The complex non-equilibrium microstructure of the processed materials occurs as a result of solid-state phase transformations, evolution of non-equilibrium phases, refined microstructures and precipitation of non-equilibrium second-phase particles during manufacturing. Thus, this complex non-equilibrium microstructure resulted specifically from multiple modes of heat, mass, and momentum transfers induced by repeated localized laser scanning. This then dictates the microstructural integrity and properties of manufactured parts [11]. The different variations in sizes of polyangular chips as well as agglomerated regions depicts the effect of created melt pools or scan area during processing. The centre of the melt pools will experience more heat than the exterior regions of the melt pool. This then affects rate at which solidification occurs and therefore creates chips of different sizes.

Figure 2 shows optical micrographs of indented areas of the as-printed WC-Co sample. These micro indentations were done on specific structures that were metallurgically visible on the optical microscope. Fig. 2a shows an indent made on the eta phase region and Fig. 2b shows an indent made on the polyangular chip. The lines showed on the indent are the scaled diagonals that are used to calculate Vickers hardness (HV) value. Table 2 shows the HV values of these two structures. It

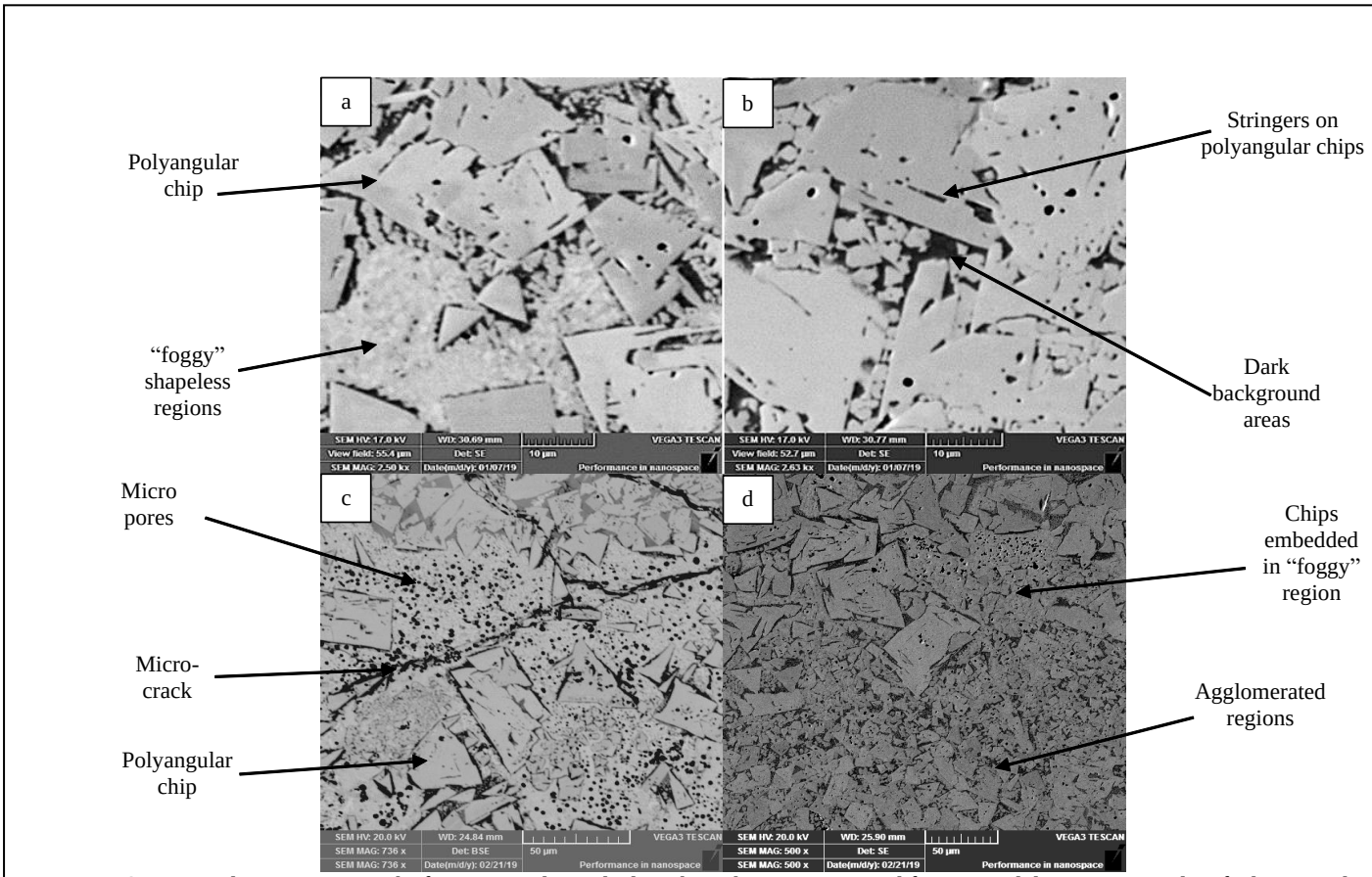

Figure 1: Scanning Electron micrographs for as-printed sample describing the microstructural features and discontinuities identified as a result of processing technique

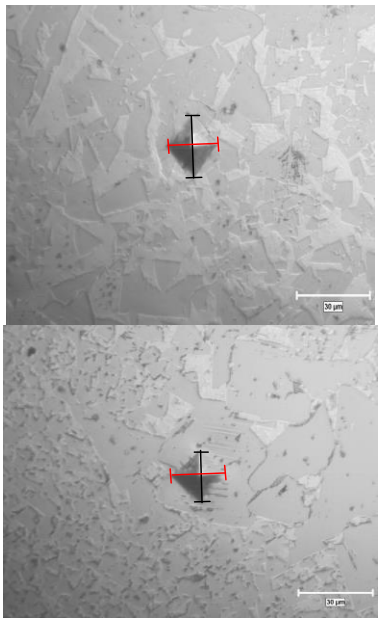

Figure 2: Optical micrographs of indents made using the Vickers hardness machine on (a) eta phase structure (b) polyangular chip observed on the as-printed WC-Co microstructure.

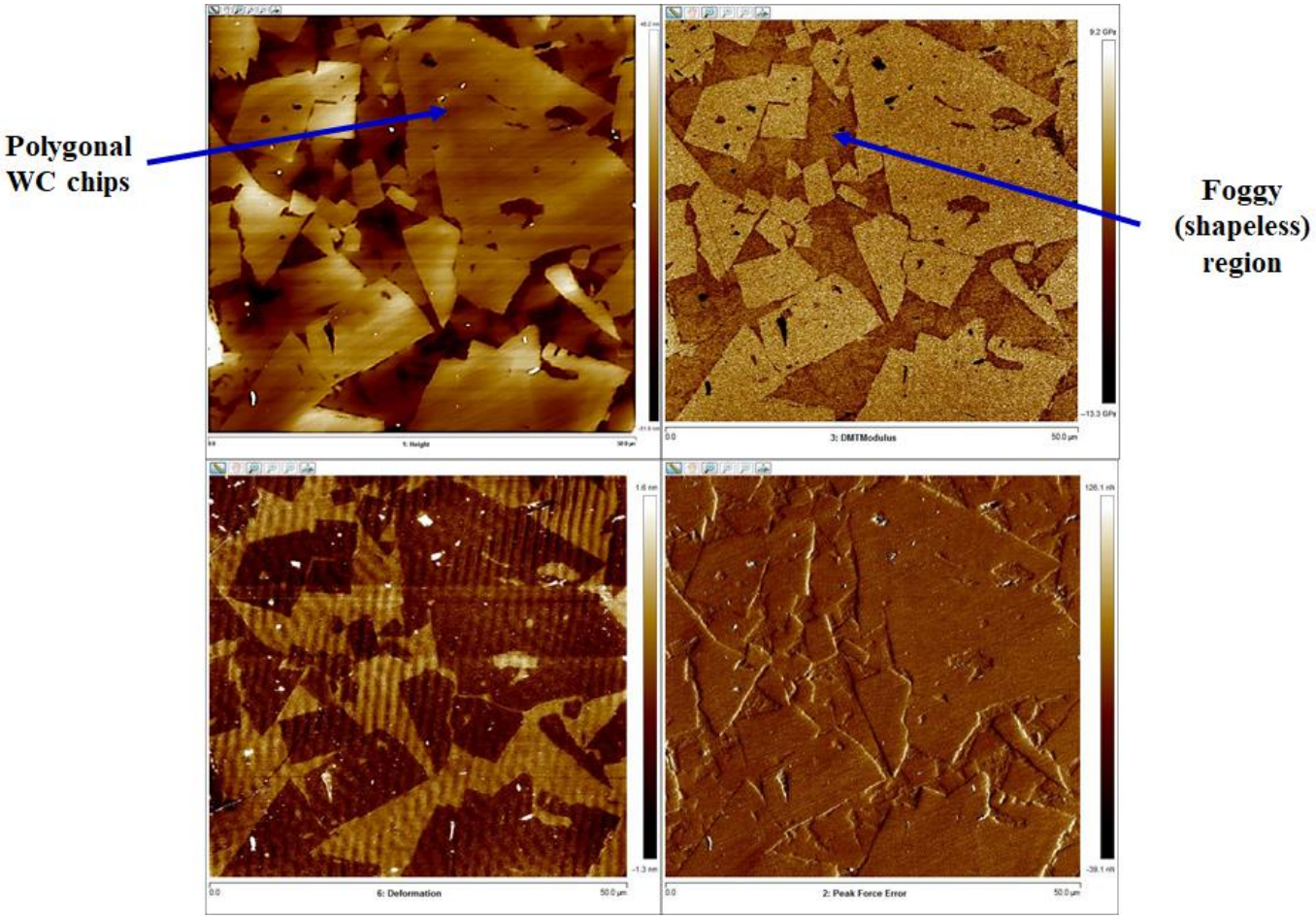

Figure 3: Nanomechanical mapping of as printed WC-Co sample showing (a) height image (b) modulus map (c) deformation mapping (d) peak force error map

is seen that the polyangular chips had a slightly higher HV value compared to the eta phase regions. An average value is shown below to give a general overview of the average micro hardness of the WC-Co sample. This is attributed to the higher volume fraction of the polyangular chips which has a higher HV value making the bulk hardness of the sample slightly higher

Structure	HV value
Eta phase regions	1104
Polyangular chip	1355
Whole sample	1302

Fig. 3 shows a topographical map, modulus map, deformation map and peak force error map as (a), (b), (c), (d for the as printed WC-Co sample. On the modulus map, the whiter the region becomes the higher the modulus value whereas on the deformation map, the whiter regions represent a softer spot because more deformation occurred at that spot. The peak force error map gives a representation of how constant the peak force, with respect to the probe, was kept during experiment. A constant peak force experiment will have an image which looks just like the topographical image of the sample. In the Fig. 3(a), a typical topographical image of the sample showed the polyangular chips are at higher elevations. This shows that the polyangular chips constitutes the matrix of the sample whereas the binder remains as the structures that are the darker areas on the image (Fig 3b). The modulus and deformation maps clearly show that the polyangular chips are harder than the eta phase regions. The dark background areas showed the softest regions as well as highest deformations. The very white spots were considered flukes which came up because of the pores on the surface of the material and therefore experienced the softest spots. Generally, mechanical strength was contributed by the volume fraction of the chips since they had higher values of modulus values. Looking at Fig. 3(d), conclusion can be made that constant peak force was kept during the experiment. Conclusively, the polyangular chips are harder than the other structures identified in the sample. Looking back at the scanning electron micrographs and hardness values, these polyangular chips can be classified as tungsten carbide (WC) chips forming the ceramic part of the composite material. The binder part is practically composed of Co however, it has W and C dissolved in it. The higher volume fraction of the WC chips makes the sample generally hard and therefore can be classified as a cemented carbide.

IV. CONCLUSION

Processing materials such as cemented carbides (WC-Co) processed using M-AM presents many challenges due to the material and complex mechanisms that occur during processing. Powder composition, processing parameters and post-processing treatments dictates the microstructural integrity and mechanical properties of the processed parts. During processing, a complex microstructure is produced which constitutes three structures namely, WC polyangular chips, eta phase regions and dark background areas. The volume fraction and spatial distribution of these structures contribute to the mechanical strength of the sample. Using nanomechanical mapping module coupled in atomic force microscopy, the WC chips are identified to be the hardest structures as compared to the other structures. Even though the eta phase regions have an equivalent mechanical strength value, it does not contribute much to the bulk properties of the material. This information would help researchers and industries alike to tailor processing parameters and post processing treatments to induce desirable structures with respect to the corresponding applications. It also shows the immense applications the Quantitative Nanomechanical Mapping mode created in the atomic force microscopy towards microstructural tailoring and analysis on the nanoscale level.

ACKNOWLEDGMENT

The authors thank the Natural Sciences and Engineering Research Council of Canada (NSERC) for the funds they provided for this investigation. The technical support provided by Mohawk College's Additive Manufacturing Resource centre is greatly appreciated.

REFERENCES

[1] Villiers Lovelock, H. L. De. 1998. "Powder/Processing/Structure Relationships in WC-Co Thermal Spray Coatings: A Review of the Published Literature." *Journal of Thermal Spray Technology* 7 (3): 357–73.

[2] Schubert, T, J Schurr, D Kolb, S Ruck, M Hofele, T Bernthaler, H Riegel, and G Schneider. 2019. "Individual Material and Process Development in Laser Based Additive Manufacturing." In Proc.SPIE. Vol. 10909. https://doi.org/10.1117/12.2508241.

[3] Fernandes C. M., Senos A., 'Cemented Carbide Phase Diagrams: A Review', Int. Journal of Refractory Metals and Hard Materials, Vol. 29 (2011), Pp. 405-418." n.d.

[4] Luo, Wenyan, Yunzhong Liu, and Junjian Shen. 2019. "Effects of Binders on the Microstructures and Mechanical Properties of Ultrafine WC-10%AlxCoCrCuFeNi Composites by Spark Plasma Sintering." *Journal of Alloys and Compounds* 791: 540–49. https://doi.org/https://doi.org/10.1016/j.jallcom.2019.03.328.

[5] García, José, Verónica Collado Ciprés, Andreas Blomqvist, and Bartek Kaplan. 2019. "Cemented Carbide Microstructures: A Review." *International Journal of Refractory Metals and Hard Materials* 80 (August 2018): 40–68. https://doi.org/10.1016/j.ijrmhm.2018.12.004.

[6] Sames, W J, F A List, S Pannala, R R Dehoff, and S S Babu. 2016. "The Metallurgy and Processing Science of Metal Additive Manufacturing." *International Materials Reviews* 61 (5): 315–60. https://doi.org/10.1080/09506608.2015.1116649.

[7] Chen, Jian, Miaojun Huang, Zak Zhigang Fang, Mark Koopman, Wei Liu, Xin Deng, Zhe Zhao, et al. 2019. "Microstructure Analysis of High-Density WC-Co Composite Prepared by One Step Selective Laser Melting." *International Journal of Refractory Metals and Hard Materials* 84 (May): 104980. https://doi.org/10.1016/j.ijrmhm.2019.104980.

[8] Fortunato, A., G. Valli, Erica Liverani, and A. Ascari. 2019. "Additive Manufacturing of WC-Co Cutting Tools for Gear Production." Lasers in Manufacturing and Materials Processing, 247–62. https://doi.org/10.1007/s40516-019-00092-0.

[9] Ku, Nicholas, John J. Pittari, Steven Kilczewski, and Andelle Kudzal. 2019. "Additive Manufacturing of Cemented Tungsten Carbide with a Cobalt-Free Alloy Binder by Selective Laser Melting for High-Hardness Applications." *Jom* 71 (4): 1535–42. https://doi.org/10.1007/s11837-019-03366-2.

[10] Uhlmann, Eckart, André Bergmann, and Witalij Gridin. 2015. "Investigation on Additive Manufacturing of Tungsten Carbide-Cobalt

by Selective Laser Melting." Procedia CIRP 35: 8–15. https://doi.org/10.1016/j.procir.2015.08.060.

[11] Mertens, A. 2016. Additive Manufacturing of Metallic Materials: An Introduction. Additive Manufacturing: Materials, Processes, Quantifications and Applications. Elsevier Inc. https://doi.org/10.1016/B978-0-12-812155-9/00003-7.

[12] Wong, Kaufui V., and Aldo Hernandez. 2012. "A Review of Additive Manufacturing." *ISRN Mechanical Engineering* 2012: 1–10. https://doi.org/10.5402/2012/208760.

[13] Kumar, S. (2018). Process chain development for additive manufacturing of cemented carbide. Journal of Manufacturing Processes, 34, 121–130. doi:10.1016/j.jmapro.2018.05.036

[14] Agyapong J, Czekanski A, Boakye-Yiadom S. Effect of heat treatment on microstructural evolution and properties of cemented carbides (WC-17Co) reinforced with 3% volume hexagonal-boron nitride (h-BN) and processed by selective laser sintering (SLS). Mater Charact 2021;174:110968.

[15] S. K. Asl, M. H. Sohi, K. Hokamoto and M. Uemura: 'Effect of heat treatment on wear behavior of HVOF thermally sprayed WC-Co coatings', Wear, 260, (11–12), 1203–1208.

[16] D.A. Stewart, P.H. Shipway, and D.G. McCartney,'Influence of heat treatment on the abrasive wear behaviour of HVOF sprayed WC-Co coatings', Surface and Coatings Technology, Vol. 105, (1998), pp. 13-24

[17] Zafar, S., Sharma, A. K., 'Microstructure and wear performance of heat-treated WC-12Co microwave clad', Vacuum, Vol. 131, (2016), pp. 213-222.

[18] Uhlmann, Eckart, André Bergmann, and Witalij Gridin. 2015. "Investigation on Additive Manufacturing of Tungsten Carbide-Cobalt by Selective Laser Melting." *Procedia CIRP* 35: 8–15. https://doi.org/10.1016/j.procir.2015.08.060.